

Two-Higgs-doublet model of type-II confronted with the LHC run-I and run-II data

Lei Wang, Xiao-Fang Han

Department of Physics, Yantai University, Yantai 264005, P. R. China

Abstract

We examine the parameter space of two-Higgs-doublet model of type-II after imposing the relevant theoretical and experimental constraints from the precision electroweak data, B -meson decays, the LHC run-I and run-II data. We find that the searches for Higgs via the $\tau\bar{\tau}$, WW , $ZZ, \gamma\gamma$, hh , hZ , HZ , AZ channels can give strong constraints on the CP-odd Higgs A and heavy CP-even Higgs H , and the parameter space excluded by each channel is respectively carved out in detail. The surviving samples are discussed in two different of regions: (i) In the SM-like coupling region of the 125 GeV Higgs, m_A is allowed to be as low as 350 GeV, and $\tan\beta$ is imposed a strong upper limit. m_H is allowed to be as low as 200 GeV for the proper $\tan\beta$, $\sin(\beta - \alpha)$ and m_A , but is required to be larger than 300 GeV for $m_A = 700$ GeV. (ii) In the wrong sign Yukawa coupling of the 125 GeV, $\tan\beta$ and $\sin(\beta - \alpha)$ can be imposed upper limits by $b\bar{b} \rightarrow A/H \rightarrow \tau\bar{\tau}$ channel and lower limits by the $A \rightarrow hZ$ channel. m_A and m_H are respectively allowed to be as low as 60 GeV and 200 GeV, but $320 \text{ GeV} < m_A < 500 \text{ GeV}$ is excluded for $m_H = 700$ GeV.

PACS numbers: 12.60.Fr, 14.80.Ec, 14.80.Bn

I. INTRODUCTION

The ongoing analyses of ATLAS and CMS show that the properties of the newly discovered 125 GeV boson are well consistent with the SM Higgs boson [1–3]. No excesses are observed in the searches for the additional exotic Higgs. The ATLAS and CMS give us plentiful limits on additional scalar state from its decay into various SM channels and some exotic decays at the LHC run-I and run-II.

The two-Higgs-doublet model (2HDM) [4] extends SM simply by adding a second $SU(2)_L$ Higgs doublet, which has very rich Higgs phenomenology, including two neutral CP-even Higgs bosons h and H , one neutral pseudoscalar A , and two charged Higgs H^\pm . According to the different Yukawa couplings, there are four types for 2HDMs which forbid the tree-level flavor changing neutral currents, the type-I [5, 6], type-II [5, 7], lepton-specific, and flipped models [8–11]. Since both the Yukawa couplings of down-type quark and lepton can be enhanced by the factor of $\tan\beta$, the type-II model can be given more stringent constraints than the other three models by the flavor observables and the LHC searches for additional Higgs. The allowed parameter space of 2HDM has been examined in light of the ATLAS and CMS searches for extra Higgses at the LHC in the literatures [12–31]

In this paper we examine the parameter space of the scenario in the type-II 2HDM considering the joint constraints from the theory, the precision electroweak data, flavor observables, the 125 GeV Higgs signal data and the searches for the additional Higgs at the LHC run-I and run-II. The 2HDM can respectively give the well fit to the 125 GeV Higgs signal data in two different regions: wrong sign Yukawa coupling and SM-like coupling. We respectively carve out the allowed parameter space in the two different regions, and obtain some interesting observables.

Our work is organized as follows. In Sec. II we introduce the 2HDM of type-II briefly. In Sec. III we perform numerical calculations. In Sec. IV, we show the allowed parameter space after imposing the relevant theoretical and experimental constraints. Finally, we give our conclusion in Sec. V.

II. TWO-HIGGS-DOUBLET MODEL OF TYPE-II

The general Higgs potential with a softly broken discrete Z_2 symmetry is written as [32]

$$\begin{aligned}
V = & m_{11}^2(\Phi_1^\dagger\Phi_1) + m_{22}^2(\Phi_2^\dagger\Phi_2) - \left[m_{12}^2(\Phi_1^\dagger\Phi_2 + \text{h.c.}) \right] \\
& + \frac{\lambda_1}{2}(\Phi_1^\dagger\Phi_1)^2 + \frac{\lambda_2}{2}(\Phi_2^\dagger\Phi_2)^2 + \lambda_3(\Phi_1^\dagger\Phi_1)(\Phi_2^\dagger\Phi_2) + \lambda_4(\Phi_1^\dagger\Phi_2)(\Phi_2^\dagger\Phi_1) \\
& + \left[\frac{\lambda_5}{2}(\Phi_1^\dagger\Phi_2)^2 + \text{h.c.} \right].
\end{aligned} \tag{1}$$

We focus on the CP-conserving model in which all λ_i and m_{12}^2 are real. The two complex scalar doublets have the hypercharge $Y = 1$:

$$\Phi_1 = \begin{pmatrix} \phi_1^+ \\ \frac{1}{\sqrt{2}}(v_1 + \phi_1^0 + ia_1) \end{pmatrix}, \quad \Phi_2 = \begin{pmatrix} \phi_2^+ \\ \frac{1}{\sqrt{2}}(v_2 + \phi_2^0 + ia_2) \end{pmatrix}. \tag{2}$$

Where v_1 and v_2 are the electroweak vacuum expectation values (VEVs) with $v^2 = v_1^2 + v_2^2 = (246 \text{ GeV})^2$, and the ratio of the two VEVs is defined as $\tan\beta = v_2/v_1$. After spontaneous electroweak symmetry breaking, there are five mass eigenstates: two neutral CP-even h and H , one neutral pseudoscalar A , and two charged scalars H^\pm .

The Yukawa interactions are written as

$$-\mathcal{L} = Y_{u2}\bar{Q}_L\tilde{\Phi}_2u_R + Y_{d1}\bar{Q}_L\Phi_1d_R + Y_{\ell1}\bar{L}_L\Phi_1e_R + \text{h.c.}, \tag{3}$$

where $Q_L^T = (u_L, d_L)$, $L_L^T = (\nu_L, l_L)$, $\tilde{\Phi}_{1,2} = i\tau_2\Phi_{1,2}^*$, and Y_{u2} , Y_{d1} and $Y_{\ell1}$ are 3×3 matrices in family space.

The Yukawa couplings of the neutral Higgs bosons normalized to the SM are given as

$$\begin{aligned}
y_h^{f_i} &= [\sin(\beta - \alpha) + \cos(\beta - \alpha)\kappa_f], \\
y_H^{f_i} &= [\cos(\beta - \alpha) - \sin(\beta - \alpha)\kappa_f], \\
y_A^{f_i} &= -i\kappa_f \text{ (for u)}, \quad y_A^{f_i} = i\kappa_f \text{ (for d, } \ell),
\end{aligned} \tag{4}$$

where $\kappa_d = \kappa_\ell \equiv -\tan\beta$ and $\kappa_u = 1/\tan\beta$.

The Yukawa interactions of the charged Higgs are given as

$$\mathcal{L}_Y = -\frac{\sqrt{2}}{v}H^+ \left\{ \bar{u}_i [\kappa_d (V_{CKM})_{ij} m_{dj} P_R - \kappa_u m_{ui} (V_{CKM})_{ij} P_L] d_j + \kappa_\ell \bar{\nu} m_\ell P_R \ell \right\} + \text{h.c.}, \tag{5}$$

where $i, j = 1, 2, 3$.

The neutral Higgs boson couplings with the gauge bosons normalized to the SM are given by

$$y_h^V = \sin(\beta - \alpha), \quad y_H^V = \cos(\beta - \alpha), \quad (6)$$

where V denotes Z or W .

The properties of the observed 125 GeV Higgs are very closed to the SM Higgs boson, which gives the strong constraints on the sector of Higgs extensions. The 2HDM can give the well fit to the 125 GeV Higgs signal data in two different regions: the SM-like coupling and the wrong sign Yukawa coupling of 125 GeV Higgs. For the former, the couplings of 125 GeV Higgs are very closed to the SM Higgs, which has a limit called the alignment limit. In the exact alignment limit [26, 33], namely $\cos(\beta - \alpha) = 0$, from Eq. (4) and Eq. (6) we find that h has the same couplings to the fermions and gauge bosons as the SM, and the heavy CP-even Higgs (H) has no couplings to the gauge bosons.

In the wrong sign Yukawa coupling region, at least one of the Yukawa couplings of the 125 GeV Higgs has the opposite sign to the coupling of gauge boson. However, their absolute values should be closed to the SM Higgs due to the constraints of 125 GeV Higgs signal data. Therefore, we can obtain

$$\begin{aligned} y_h^{f_i} &= -1 + \epsilon, \quad y_h^V \simeq 1 - 0.5 \cos^2(\beta - \alpha) \quad \text{for } \sin(\beta - \alpha) > 0 \text{ and } \cos(\beta - \alpha) > 0, \\ y_h^{f_i} &= 1 - \epsilon, \quad y_h^V \simeq -1 + 0.5 \cos^2(\beta - \alpha) \quad \text{for } \sin(\beta - \alpha) < 0 \text{ and } \cos(\beta - \alpha) > 0. \end{aligned} \quad (7)$$

Where $|\epsilon|$ and $|\cos(\beta - \alpha)|$ are much smaller than 1. From Eq. (4), we can obtain

$$\begin{aligned} \kappa_f &= \frac{-2 + \epsilon + 0.5 \cos(\beta - \alpha)^2}{\cos(\beta - \alpha)} \ll -1 \quad \text{for } \sin(\beta - \alpha) > 0 \text{ and } \cos(\beta - \alpha) > 0, \\ \kappa_f &= \frac{2 - \epsilon - 0.5 \cos(\beta - \alpha)^2}{\cos(\beta - \alpha)} \gg 1 \quad \text{for } \sin(\beta - \alpha) < 0 \text{ and } \cos(\beta - \alpha) > 0. \end{aligned} \quad (8)$$

Therefore, in the 2HDM of type-II there are the wrong sign Yukawa couplings of the down-type quark and lepton only for $\sin(\beta - \alpha) > 0$ and $\cos(\beta - \alpha) > 0$ since $\tan \beta$ is required to be larger than 1 by the B -meson observables and R_b . For the same $\sin(\beta - \alpha)$, especially for $\sin(\beta - \alpha) \rightarrow 1$, $\tan \beta$ in the wrong sign Yukawa coupling region is much larger than that of the SM-like coupling region. In other words, $\tan \beta$ has a lower bound in the wrong sign Yukawa coupling region and is allowed to be as low as 1 in the SM-like coupling. In addition, $\cos(\beta - \alpha)$ in the wrong sign Yukawa coupling is allowed to be much larger than that of the SM-like coupling due to the presence of "-2" of the numerator in the Eq. (8).

III. NUMERICAL CALCULATIONS

We take the light CP-even Higgs boson h as the SM-like Higgs, $m_h = 125$ GeV. The measurement of the branching fraction of $b \rightarrow s\gamma$ gives the stringent constraints on the charged Higgs mass of 2HDM of type-II, $m_{H^\pm} > 570$ GeV [34].

In our calculation, we consider the following observables and constraints:

- (1) Theoretical constraints and precision electroweak data. The 2HDMC [35, 36] is employed to implement the theoretical constraints from the vacuum stability, unitarity and coupling-constant perturbativity, as well as the constraints from the oblique parameters (S, T, U).
- (2) The flavor observables and R_b . We consider the constraints of B -meson decays from $B \rightarrow X_s\gamma$, Δm_{B_s} and Δm_{B_d} . SuperIso-3.4 [37] is used to calculate $B \rightarrow X_s\gamma$, and Δm_{B_s} and Δm_{B_d} are respectively calculated using the formulas in [38]. In addition, we consider the constraints of bottom quarks produced in Z decays, R_b , which is calculated following the formulas in [39, 40].
- (3) The global fit to the 125 GeV Higgs signal data. We perform the χ^2 calculation for the signal strengths of the 125 GeV Higgs in the $\mu_{ggF+ttH}(Y)$ and $\mu_{VBF+Vh}(Y)$ with Y denoting the decay mode $\gamma\gamma, ZZ, WW, \tau\bar{\tau}$ and $b\bar{b}$,

$$\chi^2(Y) = \begin{pmatrix} \mu_{ggH+ttH}(Y) - \hat{\mu}_{ggH+ttH}(Y) \\ \mu_{VBF+VH}(Y) - \hat{\mu}_{VBF+VH}(Y) \end{pmatrix}^T \begin{pmatrix} a_Y & b_Y \\ b_Y & c_Y \end{pmatrix} \times \begin{pmatrix} \mu_{ggH+ttH}(Y) - \hat{\mu}_{ggH+ttH}(Y) \\ \mu_{VBF+VH}(Y) - \hat{\mu}_{VBF+VH}(Y) \end{pmatrix}. \quad (9)$$

$\hat{\mu}_{ggH+ttH}(Y)$ and $\hat{\mu}_{VBF+VH}(Y)$ are the data best-fit values and a_Y, b_Y and c_Y are the parameters of the ellipse, which are given by the combined ATLAS and CMS experiments [3]. We pay particular attention to the surviving samples with $\chi^2 - \chi_{\min}^2 \leq 6.18$, where χ_{\min}^2 denotes the minimum of χ^2 . These samples correspond to be within the 2σ range in any two-dimension plane of the model parameters when explaining the Higgs data.

- (4) The non-observation of additional Higgs bosons. We employ HiggsBounds-4.3.1 [41, 42]

Channel	Experiment	Mass range (GeV)	Luminosity
$gg/b\bar{b} \rightarrow H/A \rightarrow \tau^+\tau^-$	ATLAS 8 TeV [45]	90-1000	19.5-20.3 fb ⁻¹
$gg/b\bar{b} \rightarrow H/A \rightarrow \tau^+\tau^-$	CMS 8 TeV [46]	90-1000	19.7 fb ⁻¹
$b\bar{b} \rightarrow H/A \rightarrow \tau^+\tau^-$	CMS 8 TeV [47]	20-80	19.7 fb ⁻¹
$gg/b\bar{b} \rightarrow H/A \rightarrow \tau^+\tau^-$	ATLAS 13 TeV [48]	200-1200	13.3 fb ⁻¹
$pp \rightarrow H/A \rightarrow \gamma\gamma$	ATLAS 13 TeV [49]	200-2400	15.4 fb ⁻¹
$gg \rightarrow H/A \rightarrow \gamma\gamma$	CMS 8+13 TeV [50]	500-4000	12.9 fb ⁻¹
$gg/VV \rightarrow H \rightarrow W^+W^-$	ATLAS 8 TeV [51]	300-1500	20.3 fb ⁻¹
$gg/VV \rightarrow H \rightarrow W^+W^- (\ell\nu\ell\nu)$	ATLAS 13 TeV [52]	300-3000	13.2 fb ⁻¹
$gg \rightarrow H \rightarrow W^+W^- (\ell\nu qq)$	ATLAS 13 TeV [53]	500-3000	13.2 fb ⁻¹
$gg/VV \rightarrow H \rightarrow ZZ$	ATLAS 8 TeV [54]	160-1000	20.3 fb ⁻¹
$gg \rightarrow H \rightarrow ZZ(\ell\ell\nu\nu)$	ATLAS 13 TeV [55]	300-1000	13.3 fb ⁻¹
$gg \rightarrow H \rightarrow ZZ(\nu\nu qq)$	ATLAS 13 TeV [56]	300-3000	13.2 fb ⁻¹
$gg/VV \rightarrow H \rightarrow ZZ(\ell\ell qq)$	ATLAS 13 TeV [56]	300-3000	13.2 fb ⁻¹
$gg/VV \rightarrow H \rightarrow ZZ(4\ell)$	ATLAS 13 TeV [57]	200-3000	14.8 fb ⁻¹
$gg \rightarrow H \rightarrow hh \rightarrow (\gamma\gamma)(b\bar{b})$	CMS 8 TeV [58]	250-1100	19.7 fb ⁻¹
$gg \rightarrow H \rightarrow hh \rightarrow (b\bar{b})(b\bar{b})$	CMS 8 TeV [59]	270-1100	17.9 fb ⁻¹
$gg \rightarrow H \rightarrow hh \rightarrow (b\bar{b})(\tau^+\tau^-)$	CMS 8 TeV [60]	260-350	19.7 fb ⁻¹
$gg \rightarrow H \rightarrow hh \rightarrow b\bar{b}b\bar{b}$	ATLAS 13 TeV [61]	300-3000	13.3 fb ⁻¹
$gg \rightarrow H \rightarrow hh \rightarrow b\bar{b}\tau^+\tau^-$	CMS 13 TeV [62]	250-900	12.9 fb ⁻¹
$gg \rightarrow A \rightarrow hZ \rightarrow (\tau^+\tau^-)(\ell\ell)$	CMS 8 TeV [60]	220-350	19.7 fb ⁻¹
$gg \rightarrow A \rightarrow hZ \rightarrow (b\bar{b})(\ell\ell)$	CMS 8 TeV [63]	225-600	19.7 fb ⁻¹
$gg \rightarrow A \rightarrow hZ \rightarrow (\tau^+\tau^-)Z$	ATLAS 8 TeV [64]	220-1000	20.3 fb ⁻¹
$gg \rightarrow A \rightarrow hZ \rightarrow (b\bar{b})Z$	ATLAS 8 TeV [64]	220-1000	20.3 fb ⁻¹
$gg/b\bar{b} \rightarrow A \rightarrow hZ \rightarrow (b\bar{b})Z$	ATLAS 13 TeV [65]	200-2000	3.2 fb ⁻¹
$gg \rightarrow A(H) \rightarrow H(A)Z \rightarrow (b\bar{b})(\ell\ell)$	CMS 8 TeV [66]	200-1000	19.8 fb ⁻¹
$gg \rightarrow A(H) \rightarrow H(A)Z \rightarrow (\tau^+\tau^-)(\ell\ell)$	CMS 8 TeV [66]	200-1000	19.8 fb ⁻¹
$gg \rightarrow A(H) \rightarrow H(A)Z \rightarrow (b\bar{b})(\ell\ell)$	CMS 13 TeV [67]	50-800	2.3 fb ⁻¹

TABLE I: The upper limits at 95% C.L. on the production cross-section times branching ratio of the processes considered in the H and A searches at the LHC run-I and run-II.

to implement the exclusion constraints from the neutral and charged Higgs searches at LEP at 95% confidence level.

At the LHC run-I and run-II the ATLAS and CMS have searched for the additional scalar state from its decay into various SM channels and some exotic decays. For the $gg \rightarrow A$ production in 2HDM of type-II, there is the destructive interference contributions of b -quark loop and top quark loop. The cross section decreases with increasing of $\tan\beta$, reaches the minimum value for the moderate value of $\tan\beta$, and is dominated by the b -quark loop for enough large value of $\tan\beta$. For the $gg \rightarrow H$ production, the cross section depends on $\sin(\beta - \alpha)$ in addition to $\tan\beta$ and m_H . We compute the cross sections for H and A in the gluon fusion and $b\bar{b}$ -associated production at NNLO in QCD via SusHi [43]. The production cross sections of H in vector boson fusion process are taken from results of the LHC Higgs Cross Section Working Group [44]. The 2HDMC is used to calculate the branching ratios of the various decay modes of H and A . A complete list of the additional Higgs searches considered by us is summarized in the Table I. For $1 \leq \tan\beta \leq 30$, the LHC searches for the heavy charged scalar can not give the constraints on the model for $m_{H^\pm} > 500$ GeV [29]. Therefore, we do not include the searches for the heavy charged Higgs.

IV. RESULTS AND DISCUSSIONS

A. The constraints from the 125 GeV Higgs signal data and the oblique parameters

The couplings of SM-like Higgs are sensitive to the parameters $\sin(\beta - \alpha)$ and $\tan\beta$. Therefore, the signal data of the 125 GeV Higgs can give the strong constraints on the two parameters. In Fig. 1, we show $\sin(\beta - \alpha)$ and $\tan\beta$ allowed by the the signal data of the 125 GeV Higgs. From Fig. 1, we find that in the SM-like coupling region of the 125 GeV Higgs, $|\sin(\beta - \alpha)|$ is required to be within the very narrow ranges, $|\sin(\beta - \alpha)| > 0.99$. However, in the wrong sign Yukawa coupling region of the 125 GeV Higgs, $\sin(\beta - \alpha)$ is allowed to be much smaller than 1, but is always positive. $\tan\beta$ is imposed a lower bound for a given value of $\sin(\beta - \alpha)$ in the wrong sign Yukwawa coupling region, such as $\tan\beta > 3$ (7) for $\sin(\beta - \alpha) = 0.87$ (0.97), while $\tan\beta$ is allowed to be as low as 1 for any value of

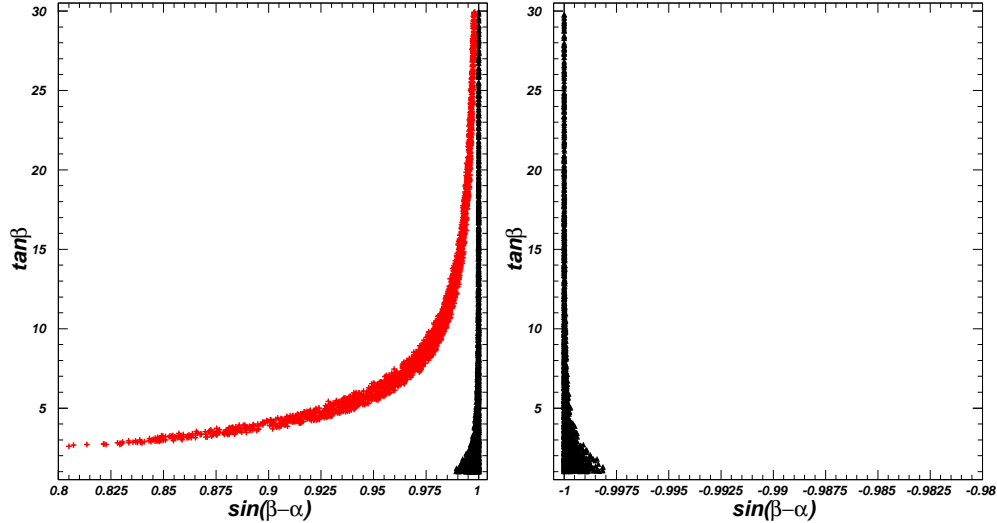


FIG. 1: The samples surviving from the constraints of the 125 GeV Higgs signal data projected on the plane of $\sin(\beta - \alpha)$ versus $\tan \beta$.

$\sin(\beta - \alpha)$ in the SM-like Higgs coupling region.

The oblique parameters S , T and U can impose the strong constraints on the 2HDM mass spectrum. In Fig. 2, we show m_H and m_A allowed by the constraints of theory and oblique parameters. The other relevant free parameters are scanned in the following range:

$$\begin{aligned}
 0.8 \leq |\sin(\beta - \alpha)| \leq 1, \quad 1 \leq \tan \beta \leq 30, \\
 570 \text{ GeV} \leq m_{H^\pm} \leq 900 \text{ GeV}, \quad -(3000 \text{ GeV})^2 \leq m_{12}^2 \leq (3000 \text{ GeV})^2.
 \end{aligned}
 \tag{10}$$

Fig. 2 shows that at least one of A and H is required to have a large mass. It is disfavored that both m_A and m_H are smaller than 440 GeV. A light A (H) favors m_H (m_A) to be around 600 GeV for $0.99 < |\sin(\beta - \alpha)| < 1$. In such range of $\sin(\beta - \alpha)$, the 125 GeV Higgs is allowed to have the SM-like coupling. With the decreasing of $|\sin(\beta - \alpha)|$, a light A favors m_H to increase. For example, for $0.8 < \sin(\beta - \alpha) < 0.9$, a light A favors m_H to be around 700 GeV. In such range of $\sin(\beta - \alpha)$, the 125 GeV Higgs is required to have the wrong-sign Yukawa coupling.

Now we carve out the allowed parameter space after imposing the joint constraints from the theory, the precision electroweak data, flavor observables, the 125 GeV Higgs signal data, and especially for the searches for the additional Higgs at the LHC run-I and run-II. The free parameters $\sin(\beta - \alpha)$, $\tan \beta$, m_{12}^2 , and m_{H^\pm} are scanned in the ranges shown in Eq. (10). If at the same time we scan m_A and m_H randomly, the constraints of each Higgs search

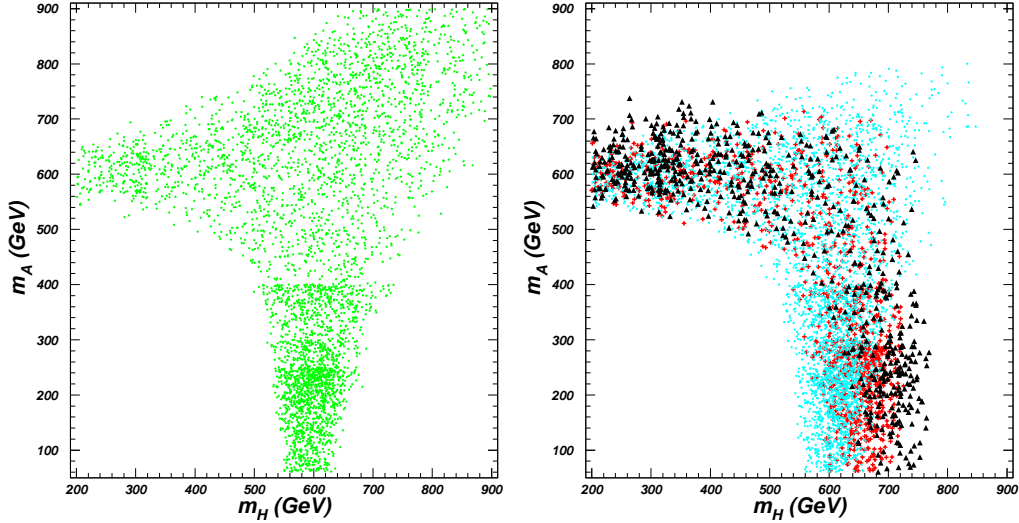


FIG. 2: Under the constraints of vacuum stability, unitarity, perturbativity, and oblique parameters, the surviving samples projected on the planes of m_H versus m_A . Left panel: $0.99 \leq |\sin(\beta - \alpha)| \leq 1$ for all the samples; Right panel: $0.95 \leq \sin(\beta - \alpha) \leq 0.99$ for the bullets (sky blue), $0.90 \leq \sin(\beta - \alpha) \leq 0.95$ for the pluses (red), and $0.80 \leq \sin(\beta - \alpha) \leq 0.90$ for the triangles (black).

channel on the property of H or A are not explicitly examined. Therefore, in each analysis we will fix one of m_A and m_H , and perform a detailed examination on the constraints of the Higgs searches channels on another Higgs. In light of the allowed Higgs mass spectrum shown in Fig. 2, we take four cases: (a) $m_H = 600$ GeV; (b) $m_H = 700$ GeV; (a) $m_A = 600$ GeV; (b) $m_A = 700$ GeV. For the four cases another Higgs is allowed to have a wide mass range including the low mass. Since a heavy Higgs can easily avoid the constraints of the Higgs searches, the light Higgs is more interesting.

B. Constraints on the CP-odd Higgs

In Fig. 3, fixing $m_H = 600$ GeV and $m_H = 700$ GeV, we project the surviving samples of the SM-like coupling region on the planes of m_A versus $\tan\beta$ and m_A versus $\sin(\beta - \alpha)$ after imposing the constraints of pre-LHC (denoting theoretical constraints, electroweak precision data, the flavor observables, R_b , the exclusion limits from searches for Higgs at LEP), the 125 GeV Higgs signal data, and the searches for additional Higgses at the LHC run-I and run-II. The upper-left panel shows that the constraints of pre-LHC and the 125 GeV Higgs

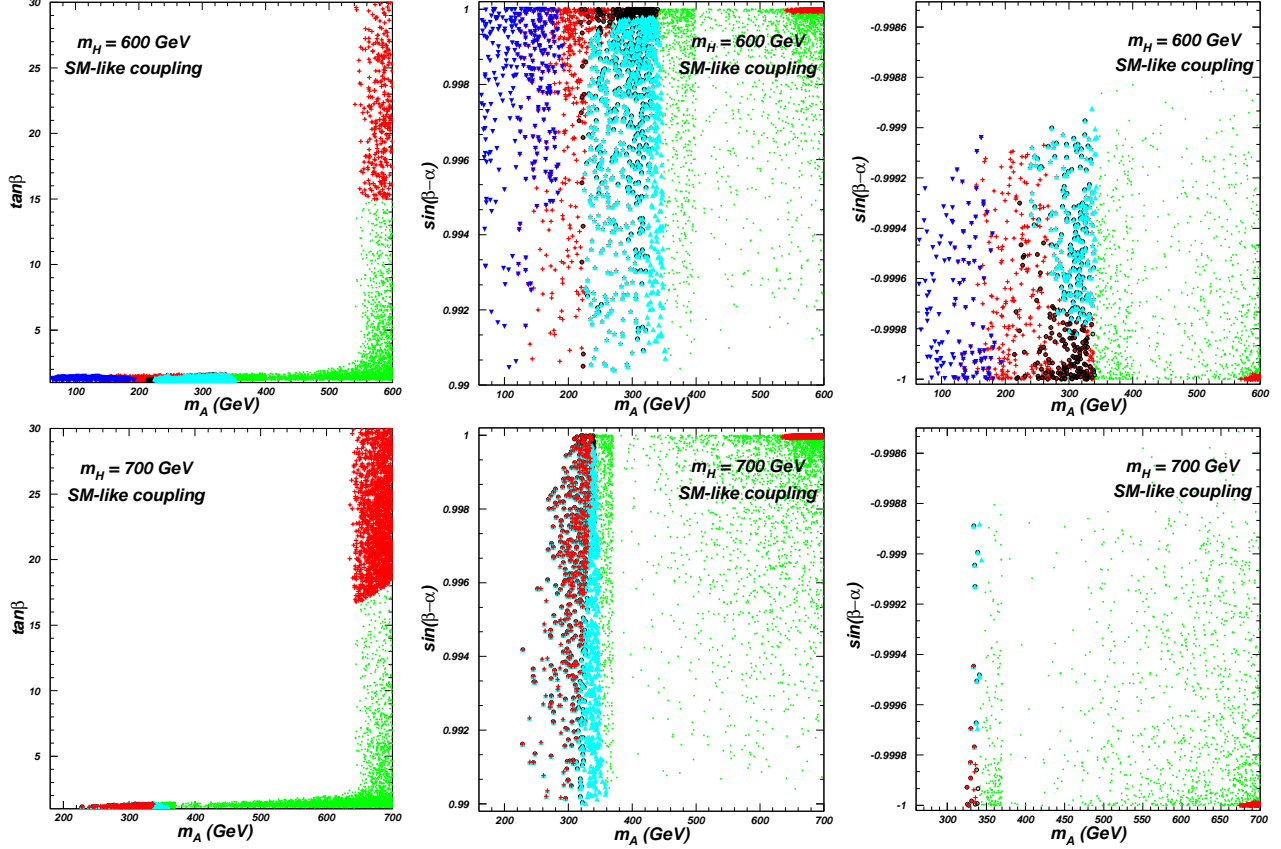


FIG. 3: The surviving samples of the SM-like coupling region projected on the planes of m_A versus $\tan \beta$ and m_A versus $\sin(\beta-\alpha)$. All the samples are allowed by the constraints of pre-LHC (denoting theoretical constrains, electroweak precision data, the flavor observables, R_b , the exclusion limits from searches for Higgs at LEP) and the 125 GeV Higgs signal data. The pluses (red), circles (black), triangles (sky blue) and inverted triangles (royal blue) are respectively excluded by the $A/H \rightarrow \tau\bar{\tau}$, $A \rightarrow \gamma\gamma$, $A \rightarrow hZ$ and $A \rightarrow HZ$ searches at the LHC run-I and run-II.

data give the strong constraints on $\tan \beta$ and m_A . $\tan \beta$ is required to be smaller than 2 for $m_A < 500$ GeV and $m_H = 600$ GeV. Further the $A \rightarrow \tau\bar{\tau}$, $A \rightarrow \gamma\gamma$, $A \rightarrow hZ$ and $H \rightarrow AZ$ channels exclude the samples in the region of $m_A < 350$ GeV. The $b\bar{b} \rightarrow A/H \rightarrow \tau\bar{\tau}$ channel can give the upper limit of $\tan \beta$, $\tan \beta < 15$ for m_A (m_H) < 600 GeV. In the SM-like Higgs coupling region, the coupling constant of $Hb\bar{b}$ is nearly the same as that of $Ab\bar{b}$. In our analysis we fix $m_H = 600$ GeV which can lead to $\tan \beta < 15$ due to the constraints of $b\bar{b} \rightarrow H \rightarrow \tau\bar{\tau}$ channel. Therefore, we do not show the parameter space $m_A > 600$ GeV although the constraints of $b\bar{b} \rightarrow A \rightarrow \tau\bar{\tau}$ on $\tan \beta$ can be relaxed.

The upper-middle and upper-right panels show that the $H \rightarrow AZ$, $A \rightarrow \gamma\gamma$, $A \rightarrow hZ$

and $A \rightarrow \tau\bar{\tau}$ searches can give the strong constraints on m_A in the closed to alignment limit. With the increasing of $|\sin(\beta - \alpha)|$, the widths of $H \rightarrow AZ$ and $A \rightarrow hZ$ increase and decrease, respectively. The constraints from the $H \rightarrow AZ$ channel become strong as $|\sin(\beta - \alpha)|$ approaches to 1, and can exclude most of samples in the range of $m_A < 200$ GeV. The $A \rightarrow hZ$ channel can exclude most of samples in the range of $220 \text{ GeV} < m_A < 350 \text{ GeV}$ except for the samples in the very closed to the alignment limit. For $350 \text{ GeV} < m_A < 540 \text{ GeV}$, the $A \rightarrow t\bar{t}$ can enhance the total width of A sizably, therefore the constraints of $H \rightarrow AZ$, $A \rightarrow \gamma\gamma$ and $A \rightarrow hZ$ channels can be satisfied. For $540 \text{ GeV} < m_A < 600 \text{ GeV}$, some samples in the very closed to the alignment limit can be excluded by the $b\bar{b} \rightarrow A/H \rightarrow \tau\bar{\tau}$ channel (also see the upper-left panel).

For $m_H = 700 \text{ GeV}$, the constraints of pre-LHC and the 125 GeV Higgs data require m_A to be larger than 220 GeV, and $\tan\beta$ to be smaller than 2 for $m_A < 640 \text{ GeV}$. The $H \rightarrow AZ$ channel can not impose the further constraints on the parameter space. The $A \rightarrow \tau\bar{\tau}$, $A \rightarrow hZ$ and $A \rightarrow \gamma\gamma$ channels can exclude $m_A < 340 \text{ GeV}$. $350 \text{ GeV} < m_A < 640 \text{ GeV}$ are allowed by the constraints of pre-LHC, the 125 GeV Higgs data and the Higgs searches at the LHC. For $640 \text{ GeV} < m_A < 700 \text{ GeV}$, the $b\bar{b} \rightarrow A \rightarrow \tau\bar{\tau}$ can exclude the exact alignment limit and require $\tan\beta$ to be smaller than 18.

Now we examine the parameter space in the wrong sign Yukawa coupling region for $m_H = 600 \text{ GeV}$ and $m_H = 700 \text{ GeV}$. In Fig. 4, we project the surviving samples on the planes of m_A versus $\tan\beta$ and m_A versus $\sin(\beta - \alpha)$ after imposing the constraints of pre-LHC, the 125 GeV Higgs signal data and the searches for additional Higgses at the LHC run-I and run-II. Since the constraints of pre-LHC and the 125 GeV Higgs signal data require $\tan\beta > 3$ in the wrong sign Yukawa coupling region, the $A \rightarrow \gamma\gamma$ and $A \rightarrow HZ$ can not give the further constraints on the parameter space.

For $m_H = 600 \text{ GeV}$ and $280 \text{ GeV} < m_A < 700 \text{ GeV}$, $\tan\beta$ and $\sin(\beta - \alpha)$ can be imposed the upper bounds by the $b\bar{b} \rightarrow A \rightarrow \tau\bar{\tau}$ channel and the lower bounds by the $A \rightarrow hZ$ channel. For example, $4.5 < \tan\beta < 9.0$ and $0.91 < \sin(\beta - \alpha) < 0.975$ for $m_A = 300 \text{ GeV}$, $8.0 < \tan\beta < 15.0$ and $0.97 < \sin(\beta - \alpha) < 0.99$ for $m_A = 400 \text{ GeV}$, $4.0 < \tan\beta < 17.0$ and $0.9 < \sin(\beta - \alpha) < 0.99$ for $m_A = 600 \text{ GeV}$. The $b\bar{b} \rightarrow A \rightarrow \tau\bar{\tau}$ channel can exclude most of samples in the range of $m_A < 200 \text{ GeV}$ except for a very narrow band of m_A around 100 GeV.

For $m_H = 700 \text{ GeV}$, the constraints of pre-LHC and the 125 GeV Higgs signal data

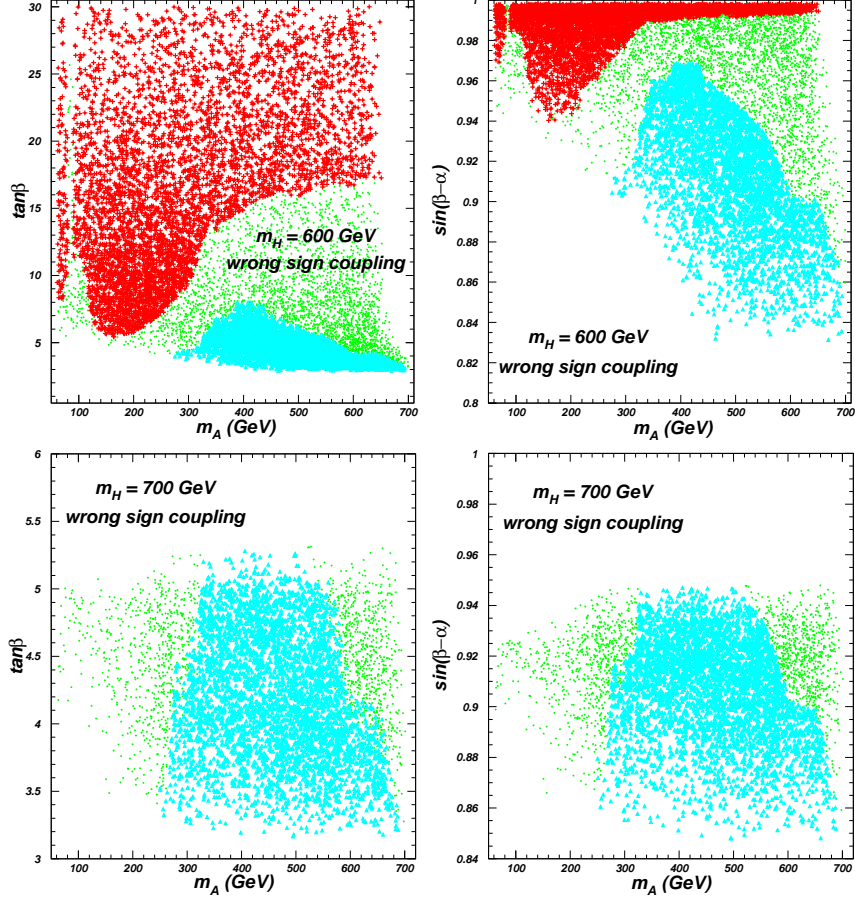


FIG. 4: The surviving samples of the wrong sign Yukawa coupling region projected on the planes of m_A versus $\tan \beta$ and m_A versus $\sin(\beta - \alpha)$. All the samples are allowed by the constraints of pre-LHC and the 125 GeV Higgs signal data. The pluses (red) and triangles (sky blue) are respectively excluded by the $A/H \rightarrow \tau\bar{\tau}$ and $A \rightarrow hZ$ searches at the LHC run-I and run-II.

require $\tan \beta < 5.5$ and $\sin(\beta - \alpha) < 0.95$. Therefore, the $b\bar{b} \rightarrow A \rightarrow \tau\bar{\tau}$ channel can not give the further constraints on the parameter space. The $A \rightarrow hZ$ channel can exclude most of samples in the range of $300 \text{ GeV} < m_A < 600 \text{ GeV}$.

C. Constraints on the heavy CP-even Higgs

Here we examine the status of the heavy CP-even Higgs after imposing the relevant theoretical and experimental constraints. In Fig. 5, fixing $m_A = 600 \text{ GeV}$ and $m_A = 700 \text{ GeV}$, we project the surviving samples on the planes of m_H versus $\tan \beta$ and m_H versus $\sin(\beta - \alpha)$. For $m_A = 600 \text{ GeV}$, the upper-left panel shows the $b\bar{b} \rightarrow H/A \rightarrow \tau\bar{\tau}$ channel gives the upper bound of $\tan \beta$, such as $\tan \beta < 6, 10$ and 15 for $m_H = 200 \text{ GeV}, 320 \text{ GeV}$

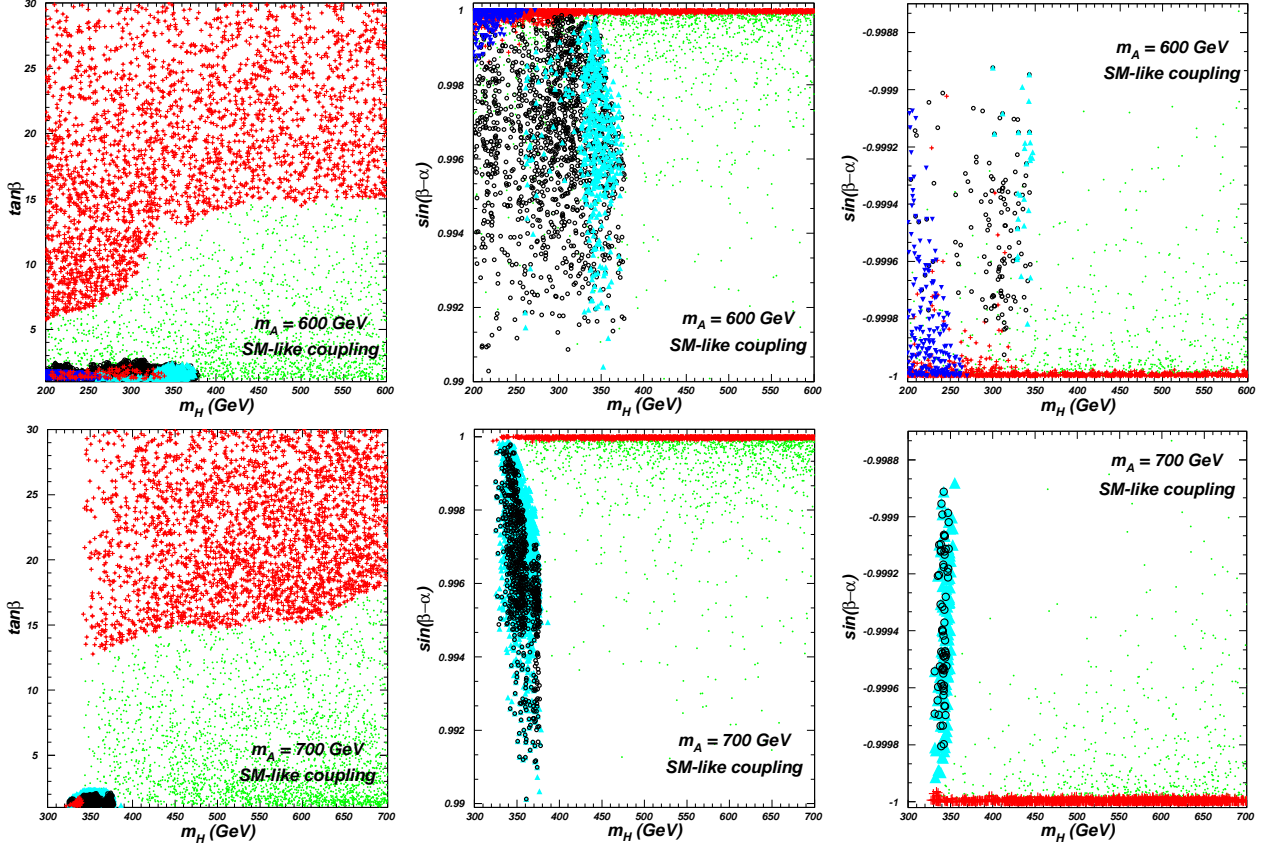


FIG. 5: The surviving samples of the SM-like coupling region projected on the planes of m_A versus $\tan\beta$ and m_A versus $\sin(\beta - \alpha)$. All the samples are allowed by the constraints of pre-LHC and the 125 GeV Higgs signal data. The pluses (red), circles (black), triangles (sky blue) and inverted triangles (royal blue) are respectively excluded by the $H/A \rightarrow \tau\bar{\tau}$, $H \rightarrow WW, ZZ, \gamma\gamma, H \rightarrow hh$, and $A \rightarrow HZ$ searches at the LHC run-I and run-II.

and 600 GeV. The $H \rightarrow \tau\bar{\tau}$, VV , $\gamma\gamma$, hh and $A \rightarrow HZ$ searches can require $\tan\beta > 2.5$ for $m_H < 380$ GeV. The proper large $\tan\beta$ can simultaneously suppress the cross sections of Higgs in the gluon fusion production and $b\bar{b}$ -quark associated production. In addition, the $H \rightarrow b\bar{b}$ can be the dominant decay mode, so that the branching ratios of $H \rightarrow VV, \gamma\gamma, hh$ will be sizably suppressed, and the constraints from these channels can be avoided.

For $m_A = 600$ GeV, the upper-middle and upper-right panels of Fig. 5 show for the proper $\tan\beta$ (see the upper-left panel), the $H/A \rightarrow \tau\bar{\tau}$, $H \rightarrow VV, \gamma\gamma, hh$, $A \rightarrow HZ$ can give the strong constraints on the m_H in the closed to the alignment limit. All the samples in the range of $m_H > 270$ GeV can satisfy the constraints of $A \rightarrow HZ$ channel. The widths

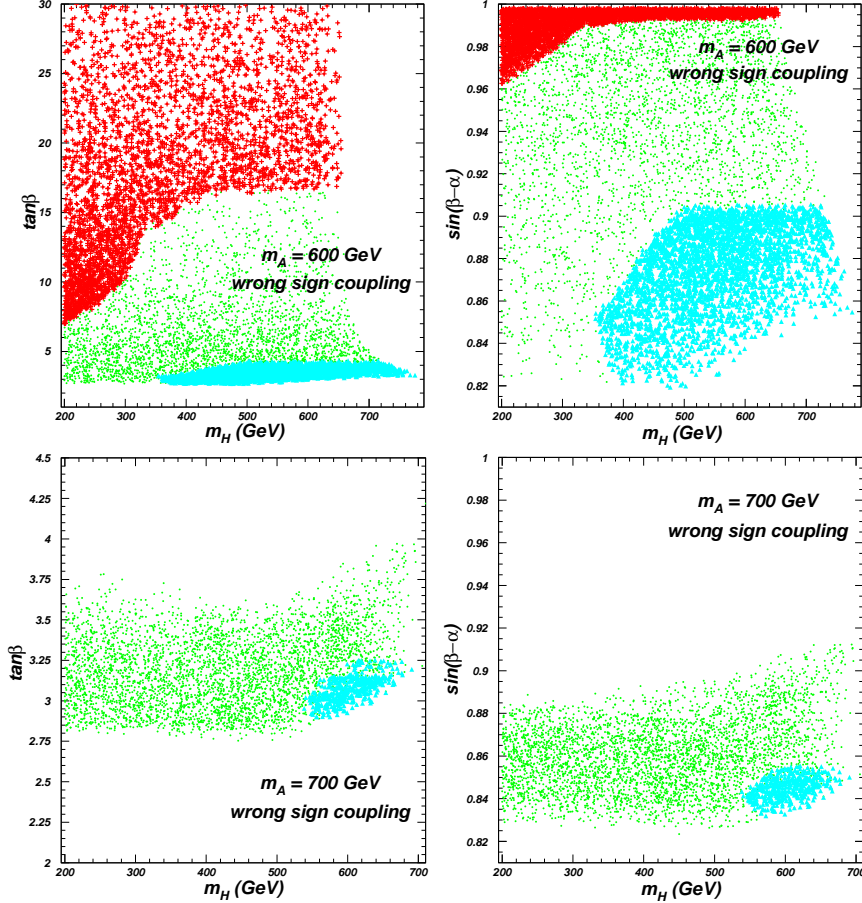


FIG. 6: The surviving samples of the wrong sign Yukawa coupling region projected on the planes of m_H versus $\tan\beta$ and m_H versus $\sin(\beta - \alpha)$. All the samples are allowed by the constraints of pre-LHC and the 125 GeV Higgs signal data. The pluses (red) and triangles (sky blue) are respectively excluded by the $H/A \rightarrow \tau\bar{\tau}$ and $A \rightarrow hZ$ searches at the LHC run-I and run-II.

of $H \rightarrow VV$, hh decrease with increasing of $|\sin(\beta - \alpha)|$ and equal to zero in the exact alignment limit. In the proper deviation from the alignment limit, the searches for these channels can exclude most of samples in the range of $m_H < 380$ GeV. With the increasing of m_H , the $H \rightarrow t\bar{t}$ can enhance the total width of H sizably, so that the constraints from $H \rightarrow VV$, $\gamma\gamma$, hh searches can be relaxed.

For $m_A = 700$ GeV, the lower-left panel of Fig. 5 shows the constraints of pre-LHC and the 125 GeV Higgs signal data require $m_H > 300$ GeV. The $A \rightarrow HZ$ channel can not give the further constraints on the parameter space. The other features of the parameter space are similar to those of $m_A = 600$ GeV.

Now we examine the parameter space in the wrong sign Yukawa coupling region for $m_A =$

600 GeV and $m_A = 700$ GeV. In Fig. 6, we project the surviving samples on the planes of m_H versus $\tan \beta$ and m_H versus $\sin(\beta - \alpha)$ after imposing the constraints of pre-LHC, the 125 GeV Higgs signal data and the searches for additional Higgses at the LHC run-I and run-II. Since the constraints of pre-LHC and the 125 GeV Higgs signal data require $\tan \beta$ to be much larger than 2 in the wrong sign Yukawa coupling region, the $H \rightarrow VV$, $\gamma\gamma$, hh and $A \rightarrow HZ$ channels can not give the further constraints on the parameter space.

For $m_A = 600$ GeV, the $b\bar{b} \rightarrow H \rightarrow \tau\bar{\tau}$ channel can impose the upper bounds on $\tan \beta$ and $\sin(\beta - \alpha)$. For example, $\tan \beta < 7.0$ and $\sin(\beta - \alpha) < 0.96$ for $m_H = 200$ GeV, $\tan \beta < 10.0$ and $\sin(\beta - \alpha) < 0.98$ for $m_H = 300$ GeV, $\tan \beta < 16.0$ and $\sin(\beta - \alpha) < 0.99$ for $m_H = 600$ GeV. All the samples in the range of $m_H < 350$ GeV can survive from the constraints of $A \rightarrow hZ$ channel. In such range of m_H , the $A \rightarrow HZ$ mode can enhance the total width of A , and lead the branching ratio of $A \rightarrow hZ$ to be suppressed. For $m_H > 350$ GeV, the $A \rightarrow hZ$ channel can exclude most of samples in the range of $\tan \beta < 4.5$ and $\sin(\beta - \alpha) < 0.905$.

For $m_A = 700$ GeV, the constraints of pre-LHC and the 125 GeV Higgs signal data require $\tan \beta < 4$ and $\sin(\beta - \alpha) < 0.92$. Therefore, the $b\bar{b} \rightarrow H \rightarrow \tau\bar{\tau}$ channel can not give the further constraints on the parameter space. The $A \rightarrow hZ$ channel can exclude most of samples in the range of $m_H > 540$ GeV, $\tan \beta < 3.25$ and $\sin(\beta - \alpha) < 0.855$.

V. CONCLUSION

We examine the parameter space of 2HDM of type-II after imposing the relevant theoretical and experimental constraints from the precision electroweak data, B -meson decays, R_b , the 125 GeV Higgs signal data, and the $H/A \rightarrow \tau\bar{\tau}$, $\gamma\gamma$, $H \rightarrow WW$, ZZ , hh , AZ , $A \rightarrow hZ$, HZ searches at the LHC run I and run II. We obtain the following observables:

(i) Status of CP-odd Higgs A . Due to the constraints of theory and oblique parameters, for m_H is around 600 GeV \sim 700 GeV, the A is allowed to have a wide range of mass, including the low mass. In the SM-like Higgs coupling region of the 125 GeV Higgs, the $A \rightarrow hZ$, $\gamma\gamma$, $\tau\bar{\tau}$ channels can exclude $140 \text{ GeV} < m_A < 350 \text{ GeV}$. For $m_H = 600$ GeV, the $H \rightarrow AZ$ can exclude most of samples in the range of $m_A < 200$ GeV. The $b\bar{b} \rightarrow A/H \rightarrow \tau\bar{\tau}$ can impose the upper limits on $\tan \beta$ and $|\sin(\beta - \alpha)|$ in the large mass range. The parameter space of $\tan \beta < 2$, $0.99 \leq \sin(\beta - \alpha) \leq 1$ and $-1 \leq \sin(\beta - \alpha) \leq -0.998$ are allowed for $m_H=600$ GeV and $350 \text{ GeV} < m_A < 540 \text{ GeV}$ as well as $m_H=700$ GeV and 350 GeV

$< m_A < 640$ GeV.

In the wrong sign Yukawa coupling region of the 125 GeV Higgs, for $m_H = 600$ GeV and $280 \text{ GeV} < m_A < 700 \text{ GeV}$, the $\tan\beta$ and $\sin(\beta - \alpha)$ can be imposed the upper bounds by the $b\bar{b} \rightarrow A \rightarrow \tau\bar{\tau}$ channel and the lower bounds by the $A \rightarrow hZ$ channel. The $b\bar{b} \rightarrow A \rightarrow \tau\bar{\tau}$ channel can exclude most of samples in the range of $m_A < 200$ GeV except for a very narrow band of m_A around 100 GeV. Compared to the case of $m_H = 600$ GeV, for $m_H = 700$ GeV, $320 \text{ GeV} < m_A < 500 \text{ GeV}$ is excluded, and the allowed parameter space is sizably narrowed since the constraints of pre-LHC and the 125 GeV Higgs signal data require $\tan\beta < 5.5$ and $\sin(\beta - \alpha) < 0.95$.

(ii) Status of heavy CP-even Higgs H . For m_A is around 600 GeV, the H is allowed to have a wide rang of mass. In the SM-like Higgs coupling region of the 125 GeV Higgs, the $b\bar{b} \rightarrow H/A \rightarrow \tau\bar{\tau}$ searches give the upper bound of $\tan\beta$, such as $\tan\beta < 6, 10$ and 15 for $m_H = 200$ GeV, 320 GeV and 600 GeV. The $H \rightarrow \tau\bar{\tau}, WW, ZZ, \gamma\gamma, hh$ channels require $\tan\beta > 2.5$ for $m_H < 380$ GeV. For $m_A = 600$ GeV, the $A \rightarrow HZ$ channel can exclude most of samples in the range of $m_H < 270$ GeV. For the proper $\tan\beta$ and $\sin(\beta - \alpha)$, m_H is allowed to be as low as 200 GeV for $m_A = 600$ GeV and 300 GeV for $m_A = 700$ GeV.

In the wrong sign Yukawa coupling region of the 125 GeV Higgs, the $b\bar{b} \rightarrow H \rightarrow \tau\bar{\tau}$ channel can impose the upper bounds on $\tan\beta$ and $\sin(\beta - \alpha)$. For $m_A = 600$ GeV, the $A \rightarrow hZ$ channel can exclude most of samples in the range of $\tan\beta < 4.5, \sin(\beta - \alpha) < 0.905$ and $m_H > 350$ GeV. Compared to the case of $m_A = 600$ GeV, for $m_A = 700$ GeV, the allowed parameter space are sizably narrowed since the constraints of pre-LHC and the 125 GeV Higgs signal data require $\tan\beta < 4$ and $\sin(\beta - \alpha) < 0.92$. For the proper $\tan\beta$ and $\sin(\beta - \alpha)$, m_H is allowed to be as low as 200 GeV for both $m_A = 600$ GeV and $m_A = 700$ GeV.

Acknowledgment

We thank Qing-Hong Cao and Ye Chen for helpful discussions. This work is supported by the National Natural Science Foundation of China under grant No. 11575152.

[1] **CMS** Collaboration, S. Chatrchyan et al., Phys. Lett. B **716**, 30 (2012).

- [2] **ATLAS** Collaboration, G. Aad et al., Phys. Lett. B **716**, 1 (2012).
- [3] **ATLAS** and **CMS** Collaborations, JHEP **1608**, (2016) 045.
- [4] T. D. Lee, Phys. Rev. D **8**, 1226 (1973).
- [5] H. E. Haber, G. L. Kane and T. Sterling, Nucl. Phys. B **161**, 493 (1979).
- [6] L. J. Hall and M. B. Wise, Nucl. Phys. B **187**, 397 (1981).
- [7] J. F. Donoghue and L. F. Li, Phys. Rev. D **19**, 945 (1979).
- [8] V. D. Barger, J. L. Hewett and R. J. N. Phillips, Phys. Rev. D **41**, 3421 (1990).
- [9] Y. Grossman, Nucl. Phys. B **426**, 3 (1994).
- [10] A. G. Akeroyd and W. J. Stirling, Nucl. Phys. B **447**, 3 (1995).
- [11] A. G. Akeroyd, Phys. Lett. B **377**, 95 (1996).
- [12] A. Celis, V. Ilisie and A. Pich, JHEP **1307**, 053 (2013).
- [13] B. Grinstein, P. Uttayarat, JHEP **1306**, 094 (2013), [Erratum-ibid. 1309, 110 (2013)].
- [14] C. -Y. Chen, S. Dawson, M. Sher, Phys. Rev. D **88**, 015018 (2013).
- [15] N. Craig, J. Galloway and S. Thomas, arXiv:1305.2424.
- [16] O. Eberhardt, U. Nierste and M. Wiebusch, JHEP **1307**, 118 (2013).
- [17] B. Dumont, J. F. Gunion, Y. Jiang and S. Kraml, Phys. Rev. D **90**, 035021 (2014).
- [18] E. J. Chun, Z. Kang, M. Takeuchi, Y.-L. S. Tsai, JHEP **1511**, 099 (2015).
- [19] S.-H. Zhu, Nucl. Part. Phys. Proc. **273-275**, 716-720 (2016).
- [20] D. Chowdhury, O. Eberhardt, JHEP **1511**, 052 (2015).
- [21] V. Cacchio, D. Chowdhury, O. Eberhardt, C. W. Murphy, JHEP **1611**, 026 (2016).
- [22] N. Chakrabarty, U. K. Dey, B. Mukhopadhyaya, JHEP **1412**, 166 (2014).
- [23] J. Baglio, O. Eberhardt, U. Nierste, M. Wiebusch, Phys. Rev. D **90**, 015008 (2014).
- [24] J. Bernon, B. Dumont and S. Kraml, Phys. Rev. D **90**, 071301 (2014).
- [25] N. Craig, F. DEramo, P. Draper, S. Thomas, H. Zhang, JHEP **1506**, 137 (2015).
- [26] J. Bernon, J. F. Gunion, H. E. Haber, Y. Jiang, S. Kraml, Phys. Rev. D **92**, 075004 (2015).
- [27] F. Kling, A. Pyarelal and S. Su, JHEP **1511**, 051 (2015).
- [28] A. G. Akeroyd et al., arXiv:1607.01320.
- [29] S. Moretti, arXiv:1612.02063.
- [30] G. C. Dorsch, S. J. Huber, K. Mimasu, J. M. No, Phys. Rev. D **93**, 115033 (2016).
- [31] F. Kling, J. M. No, S. Su, JHEP **1609**, 093 (2016).
- [32] R. A. Battye, G. D. Brawn, A. Pilaftsis, JHEP **1108**, 020 (2011).

- [33] P. S. Bhupal Dev, A. Pilaftsis, JHEP **12**, 024 (2014).
- [34] Heavy Flavor Averaging Group, arXiv:1612.07233; M. Misiak, M. Steinhauser, arXiv:1702.04571.
- [35] D. Eriksson, J. Rathsman, O. Stål, Comput. Phys. Commun. **181**, 189 (2010).
- [36] D. Eriksson, J. Rathsman, O. Stål, Comput. Phys. Commun. **181**, 833 (2010).
- [37] F. Mahmoudi, Comput. Phys. Commun. **180**, 1579-1673 (2009).
- [38] C. Q. Geng and J. N. Ng, Phys. Rev. D **38**, 2857 (1988) [Erratum-ibid. D 41, 1715 (1990)].
- [39] H. E. Haber, H. E. Logan, Phys. Rev. D **62**, 015011 (2010).
- [40] G. Degrossi, P. Slavich, Phys. Rev. D **81**, 075001 (2010).
- [41] P. Bechtle, O. Brein, S. Heinemeyer, G. Weiglein, K. E. Williams, Comput. Phys. Commun. **181**, 138-167 (2010).
- [42] P. Bechtle, O. Brein, S. Heinemeyer, O. Stål, T. Stefaniak, G. Weiglein, K. E. Williams, Eur. Phys. Jour. C **74**, 2693 (2014).
- [43] R. V. Harlander, S. Liebler and H. Mantler, Comput. Phys. Commun. **184**, 1605 (2013).
- [44] S. Heinemeyer et al. [LHC Higgs Cross Section Working Group Collaboration], arXiv:1307.1347.
- [45] **ATLAS** Collaboration, G. Aad *et al.*, “Search for neutral Higgs bosons of the minimal supersymmetric standard model in pp collisions at $\sqrt{s} = 8$ TeV with the ATLAS detector,” JHEP **11**, 056 (2014).
- [46] **CMS** Collaboration, “Search for additional neutral Higgs bosons decaying to a pair of tau leptons in pp collisions at $\sqrt{s} = 7$ and 8 TeV,” CMS-PAS-HIG-14-029.
- [47] **CMS** Collaboration, “Search for a low-mass pseudoscalar Higgs boson produced in association with a $b\bar{b}$ pair in pp collisions at $\sqrt{s} = 8$ TeV,” arXiv:1511.03610.
- [48] **ATLAS** Collaboration, “Search for Minimal Supersymmetric Standard Model Higgs Bosons H/A in the $\tau\tau$ final state in up to 13.3 fb^{-1} of pp collisions at $\sqrt{s} = 13$ TeV with the ATLAS Detector,” ATLAS-CONF-2016-085.
- [49] **ATLAS** Collaboration, “Search for scalar diphoton resonances with 15.4 fb^{-1} of data collected at $\sqrt{s} = 13$ TeV in 2015 and 2016 with the ATLAS detector,” ATLAS-CONF-2016-059.
- [50] **CMS** Collaboration, “Search for resonant production of high mass photon pairs using 12.9 fb^{-1} of proton-proton collisions at $\sqrt{s} = 13$ TeV and combined interpretation of searches at 8 and 13 TeV,” CMS-PAS-EXO-16-027.

- [51] **ATLAS** Collaboration, G. Aad *et al.*, “Search for a high-mass Higgs boson decaying to a W boson pair in pp collisions at $\sqrt{s} = 8$ TeV with the ATLAS detector,” *JHEP* **01**, (2016) 032.
- [52] **ATLAS** collaboration, “Search for a high-mass Higgs boson decaying to a pair of W bosons in pp collisions at $\sqrt{s}=13$ TeV with the ATLAS detector,” ATLAS-CONF-2016-074.
- [53] **ATLAS** Collaboration, G. Aad *et al.*, “Search for diboson resonance production in the $\ell\nu qq$ final state using pp collisions at $\sqrt{s} = 13$ TeV with the ATLAS detector at the LHC,” ATLAS-CONF-2016-062.
- [54] **ATLAS** Collaboration, G. Aad *et al.*, “Search for an additional, heavy Higgs boson in the $H \rightarrow ZZ$ decay channel at $\sqrt{s} = 8$ TeV in pp collision data with the ATLAS detector,” *Eur. Phys. Jour. C* **76**, 45 (2016).
- [55] **ATLAS** Collaboration, “Search for new phenomena in the $Z(\rightarrow \ell\ell) + E_{\text{T}}^{\text{miss}}$ final state at $\sqrt{s} = 13$ TeV with the ATLAS detector,” ATLAS-CONF-2016-056.
- [56] **ATLAS** Collaboration, “Searches for heavy ZZ and ZW resonances in the $\ell\ell qq$ and $\nu\nu qq$ final states in pp collisions at $\sqrt{s} = 13$ TeV with the ATLAS detector,” ATLAS-CONF-2016-082.
- [57] **ATLAS** Collaboration, “Study of the Higgs boson properties and search for high-mass scalar resonances in the $H \rightarrow ZZ^* \rightarrow 4\ell$ decay channel at $\sqrt{s} = 13$ TeV with the ATLAS detector,” ATLAS-CONF-2016-079.
- [58] **CMS** Collaboration, V. Khachatryan *et al.*, “Search for two Higgs bosons in final states containing two photons and two bottom quarks,” arXiv:1603.06896.
- [59] **CMS** Collaboration, V. Khachatryan *et al.*, “Search for resonant pair production of Higgs bosons decaying to two bottom quark–antiquark pairs in proton–proton collisions at 8 TeV,” *Phys. Lett. B* **749**, 560-582 (2015).
- [60] **CMS** Collaboration, V. Khachatryan *et al.*, “Searches for a heavy scalar boson H decaying to a pair of 125 GeV Higgs bosons hh or for a heavy pseudoscalar boson A decaying to Zh , in the final states with $h \rightarrow \tau\tau$,” *Phys. Lett. B* **755**, 217-244 (2016).
- [61] **ATLAS** Collaboration, “Search for pair production of Higgs bosons in the $b\bar{b}b\bar{b}$ final state using proton–proton collisions at $\sqrt{s} = 13$ TeV with the ATLAS detector,” ATLAS-CONF-2016-049.
- [62] **CMS** Collaboration, “Search for resonant Higgs boson pair production in the $b\bar{b}\tau^+\tau^-$ final state using 2016 data,” CMS-PAS-HIG-16-029.

- [63] **CMS** Collaboration, V. Khachatryan *et al.*, “Search for a pseudoscalar boson decaying into a Z boson and the 125 GeV Higgs boson in $\ell^+\ell^-b\bar{b}$ final states,” Phys. Lett. B **748**, 221-243 (2015).
- [64] **ATLAS** Collaboration, G. Aad *et al.*, “Search for a CP-odd Higgs boson decaying to Zh in pp collisions at $\sqrt{s} = 8$ TeV with the ATLAS detector,” Phys. Lett. B **744**, 163-183 (2015).
- [65] **ATLAS** Collaboration, “Search for a CP-odd Higgs boson decaying to Zh in pp collisions at $s = 13$ TeV with the ATLAS detector,” ATLAS-CONF-2016-015.
- [66] **CMS** Collaboration, V. Khachatryan *et al.*, “Search for neutral resonances decaying into a Z boson and a pair of b jets or τ leptons,” arXiv:1603.02991.
- [67] **CMS** Collaboration, V. Khachatryan *et al.*, “Search for $pp \rightarrow H \rightarrow ZA \rightarrow \ell^+\ell^-bb$ with 2015 data,” CMS-PAS-HIG-16-010.